Cyclization kinetics of Gaussian semiflexible polymer chains

T. Guérin,[1,2] M. Dolgushev,[3] O. Bénichou,[1] R. Voituriez,[1] and A. Blumen[3]

[1]*Laboratoire de Physique Théorique de la Matière Condensée, CNRS/UPMC, 4 Place Jussieu, 75005 Paris, France*

[2]*Laboratoire Ondes et Matière d'Aquitaine, University of Bordeaux, Unité Mixte de Recherche 5798, CNRS, F-33400 Talence, France*

[3]*Theoretical Polymer Physics, University of Freiburg, Hermann-Herder-Str. 3, D-79104 Freiburg, Germany*

(Received 26 May 2014; revised manuscript received 22 September 2014; published 12 November 2014)

We consider the dynamics and the cyclization kinetics of Gaussian semiflexible chains, in which the interaction potential tends to align successive bonds. We provide asymptotic expressions for the cyclization time, for the eigenvalues and eigenfunctions, and for the mean square displacement at all time and length scales, with explicit dependence on the capture radius, on the positions of the reactive monomers in the chain, and on the finite number of beads. For the cyclization kinetics, we take into account non-Markovian effects by calculating the distribution of reactive conformations of the polymer, which are not taken into account in the classical Wilemski-Fixman theory. Comparison with numerical simulations confirms the accuracy of this non-Markovian theory.

DOI: 10.1103/PhysRevE.90.052601 PACS number(s): 82.35.−x, 05.40.−a

I. INTRODUCTION

The theoretical description of reactions involving polymer chains has attracted growing interest over the last few years. A prototypical example is given by cylization reactions, which are ubiquitous in chemistry and biochemistry: examples range from the formation of RNA hairpins [1–4], the folding of polypeptide chains [5–7], to the formation of loops in DNA strands, which play a role for the regulation of gene expression [8] and were proposed to be used as a tool to measure polymer mechanical properties [9,10]. However, even in the simplest example of the Rouse chain, the theoretical determination of the mean reaction time is a nontrivial problem due to the multiple time scales involved in the polymer dynamics [11]. An important step has been provided by the Wilemski-Fixman approach [12,13], which, however, implicitly relies on an effective Markovian description of the dynamics of the reactive monomers. Recently several extensions have been proposed [14–19], and in particular it was shown that memory effects, neglected so far in the available Markovian approaches, could be quantitatively important [19–21]. We recall that so far these analytical descriptions were essentially restricted to flexible chains, i.e., polymers for which the bending stiffness was neglected.

Semiflexible polymers are characterized by a finite bending stiffness, which implies the existence of an additional length scale in the problem, namely, the persistence length. Semiflexible polymers behave as flexible polymers when their length is much longer than the persistence length and are similar to rigid rods at smaller length scales. They are ubiquitous and play an essential role in biology: a number of biological polymers, such as the components of the cytoskeleton (actin and microtubules), or nucleic acid DNA and RNA chains are often modeled as wormlike chains [22–24]. A number of studies have characterized very well the equilibrium properties of semiflexible polymers, such as the distribution of the end-to-end vector, or the equilibrium contact probability between two monomers of the same chain, called the cyclization factor [8,22,25]. The dynamic properties of semiflexible chains [22,26,27], and their impact on the cyclization kinetics, are far less understood than their equilibrium properties, in part because of the multiple length scales present in the problem. One existing analytical approach to the calculation of the cyclization time consists in considering a simplified dynamics involving only one degree of freedom [28,29]. Interestingly, recent Brownian dynamics simulations [30] indicate that this approach fails to predict the cyclization time, leading to the conclusion that the collective dynamics of all the monomers have a significant impact on the reaction time.

In this paper, we focus on the impact of the collective dynamics of the monomers on the cyclization kinetics in the framework of a Gaussian model [31,32] of semiflexible polymer dynamics that takes into account all time scales (see Fig. 1). This Gaussian model is a simplified version of the wormlike chain model, where the inextensibility constraint is satisfied only on average. This arbitrary assumption is questionable, but this model predicts almost exact asymptotic forms for a number of quantities such as the intrinsinc viscosity and the relaxation times [31], which justifies the use of this model as a first step to understand cyclization in semiflexible chains. Earlier studies of cyclization kinetics using this model have dealt with simplified geometries [33,34], or with numerical integration of the Wilemski-Fixman equations [35,36]. In this context, the first goal of the present work is to identify all the regimes of cyclization kinetics that are present in this model, in order to understand the impact of the position of the reactive monomers, the capture radius, or the polymer length. As mentioned above, the fact that the motion of the end-to-end vector displays memory is another aspect that is neglected in existing theoretical approaches [28,29,33–36]. Our second goal in this paper will be to explicitly characterize the non-Markovian effects in all the regimes by using the method introduced in Refs. [19,21]. Memory effects will be found to be quantitatively important in the regime controlled by the small length scales bending fluctuations of the chain.

The paper is organized as follows. In Sec. II, we introduce the Gaussian model of semiflexible chains, first in the discrete picture of beads linked by springs that tend to align with their neighbors, and second in the associated continuous model, more suitable for analytical calculations. Then, in Sec. III, we derive explicitly all the asymptotic regimes present in the model. In Sec. IV, we then identify all the regimes of the cyclization time, first in the Wilemski-Fixman approximation (Sec. IV A), where one implicitly neglects the presence of

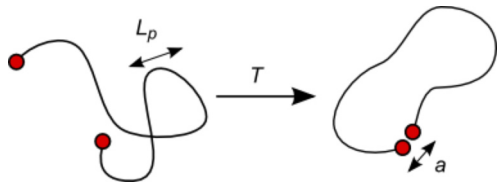

FIG. 1. (Color online) In this paper we calculate the mean first cyclization time $\langle \mathbf{T} \rangle$, defined as the mean first time that two given monomers of a Gaussian semiflexible chain, here represented at the chain ends, reach a relative distance smaller than a capture radius a.

memory in the motion of the relative vector between the reactive monomers. In Sec. IV B, we identify the magnitude of the memory effects in all the different regimes. Finally, in Sec. IV C we report the results of numerical simulations, which confirm the accuracy of our approach. We discuss our results and the hypotheses made in the conclusion.

II. DISCRETE AND CONTINUOUS GAUSSIAN MODELS OF SEMIFLEXIBLE CHAINS

A. Discrete model

We first introduce the discrete model of Gaussian semiflexible chains. The chain is represented by N beads moving in a three-dimensional space. We call $\mathbf{r}_i(t)$ $(1 \leqslant i \leqslant N)$ the position of the center of the ith bead at time t, where quantities in bold represent three-dimensional vectors. Two successive beads are linked by a bond $\mathbf{d}_i = \mathbf{r}_{i+1} - \mathbf{r}_i$ $(1 \leqslant i \leqslant N-1)$. We consider the dynamic model introduced by Bixon and Zwanzig [31], which satisfies the following requirements: (i) the mean square length of each bond at equilibrium is $\langle \mathbf{d}_i^2 \rangle_{\rm eq} = b^2$, (ii) the correlations between different bonds at equilibrium follow the freely rotating conditions, $\langle \mathbf{d}_i . \mathbf{d}_{i+p} \rangle_{\rm eq} = g^p b^2$ for any integer p, where g is a dimensionless stiffness parameter satisfying $0 \leqslant g < 1$, and (iii) the potential is quadratic. These conditions lead to the potential [31]

$$V(\{\mathbf{d}_i\}) = \frac{3k_BT}{2b^2(1-g^2)}\Bigg[\sum_{i=1}^{N-1}(1+g^2)\mathbf{d}_i^2 - g^2\left(\mathbf{d}_1^2 + \mathbf{d}_{N-1}^2\right) - 2g\sum_{i=1}^{N-2}\mathbf{d}_i.\mathbf{d}_{i+1}\Bigg]. \quad (1)$$

In this expression, the terms $-g\mathbf{d}_i.\mathbf{d}_{i+1}$ indicate an energy penalty when two successive bonds are not aligned. When $g = 0$, one recovers the Rouse model [37] of flexible chains, whereas for $g \to 1$ the polymer becomes much stiffer. In Eq. (1), the particular terms for the first and last bonds are important to ensure that the constraint $\langle \mathbf{d}_i^2 \rangle = b^2$ is satisfied everywhere along the chain. To derive the equations of motion, we assume that each bead experiences a friction force $-\zeta\,\partial_t \mathbf{r}_i$, a stochastic force $\mathbf{f}_i(t)$ due to the solvent temperature, and the forces $\mathbf{F}_i = -\partial_{\mathbf{r}_i} V$ that are derived from the potential (1) and come from the interactions between neighboring beads in the chain. Then the equations of motion of the chain are given in Langevin form by

$$\partial_t \mathbf{r}_i = -\zeta^{-1}\boldsymbol{\nabla}_i V + \mathbf{f}_i(t), \quad (2)$$

where $\boldsymbol{\nabla}_i = \partial/\partial\mathbf{r}_i$ and the forces $\mathbf{f}_i(t)$ are uncorrelated white noise sources, whose amplitudes obey $\langle f_{i,\alpha}(t) f_{j,\beta}(t') \rangle = 2k_BT\zeta^{-1}\delta(t-t')\delta_{\alpha\beta}\delta_{ij}$, where α and β represent the spatial coordinates x, y, z. Note that the hydrodynamic interactions are not taken into account in Eq. (2), and that the stochastic process $\{\mathbf{r}_i(t)\}$ is Gaussian, since the forces $\mathbf{F}_i = -\partial_{\mathbf{r}_i} V$ are linear functions of the bead positions.

B. Continuous model

In order to perform analytical calculations, it is useful to introduce the continuous form of the model. We introduce the polymer contour length $L = Nb$, its persistence length $L_p = b/(1-g)$, and the friction coefficient per unit length, $\gamma = \zeta/b$, which has the dimension of a viscosity. We call $\ell = L/L_p$ the ratio of the contour length over the persistence length: $\ell \ll 1$ corresponds to a stiff polymer, whereas for $\ell \gg 1$ the polymer is flexible and is much longer than its persistence length. We also introduce s_i, the position in the chain of the ith monomer, defined by $s_i = [(i-1/2)b - L/2]$, with $-L/2 \leqslant s_i \leqslant L/2$. The continuous model is obtained by taking the limit $N \to \infty$ while the parameters L_p, L and γ remain constant, which implies that $b \to 0$ and $g \to 1$. The continuous form of the Langevin equation (2) has been determined by Harnau *et al.* [32] and reads

$$\partial_t \mathbf{r}(s,t) = \tau_c^{-1} L_p^2\left(-L_p^2\partial_s^4 + \partial_s^2\right)\mathbf{r}(s,t) + \mathbf{f}(t,s), \quad (3)$$

$$\langle f_\alpha(s,t) f_\beta(s',t') \rangle = 2k_BT\gamma^{-1}\delta(t-t')\delta(s-s')\delta_{\alpha\beta}, \quad (4)$$

where we have defined the characteristic time τ_c:

$$\tau_c = \frac{2\gamma L_p^3}{3k_BT}. \quad (5)$$

The time τ_c is of the order of the rotational relaxation time of a polymer of length L_p. The fourth derivative $\partial_s^4\mathbf{r}$ in Eq. (3) accounts for the bending rigidity, while the term $\partial_s^2\mathbf{r}$ accounts for the polymer entropic stiffness. The equation of motion (3) must also be supplemented with a set of boundary conditions [32] that directly arise from the presence of the particular terms for the first and last bonds in the potential (1):

$$\begin{aligned}\left(L_p\partial_s^2 - \partial_s\right)\mathbf{r}(s,t)|_{s=-L/2} &= 0,\\ \left(L_p\partial_s^2 + \partial_s\right)\mathbf{r}(s,t)|_{s=L/2} &= 0,\\ \left(L_p^2\partial_s^3 - \partial_s\right)\mathbf{r}(s,t)|_{s=-L/2} &= 0,\\ \left(L_p^2\partial_s^3 - \partial_s\right)\mathbf{r}(s,t)|_{s=L/2} &= 0.\end{aligned} \quad (6)$$

The equations of motion (3) with the boundary conditions (6) ensure that the inextensibility constraint $\langle(\partial_s\mathbf{r})^2\rangle = 1$ is satisfied on average, and that the equilibrium average square distance between two monomers on the chain have the same value as for the wormlike chain model [38].

III. DYNAMICS OF THE RELATIVE DISTANCE BETWEEN TWO MONOMERS

A. Eigenvalue expansion

We introduce the vector joining two monomers at positions s_1 and s_2 along the chain

$$\mathbf{R}(t) = \mathbf{r}(s_1,t) - \mathbf{r}(s_2,t). \tag{7}$$

In this section, we focus on the description of the dynamics of the vector $\mathbf{R}(t)$ in various limiting cases, in order to identify all the dynamical regimes present in the model. The variable $\mathbf{R}(t)$ will be conveniently expressed in terms of normal modes. We introduce the eigenfunctions $g_q(s)$ and eigenvalues λ_q (with $\lambda_0 = 0 < \lambda_1 < \lambda_2 < \cdots$), that satisfy

$$-L_p^4\ \partial_s^4 g_q(s) + L_p^2\ \partial_s^2 g_q(s) = -\lambda_q \tau_c\ g_q(s), \tag{8}$$

with $g_q(s)$ satisfying the boundary conditions (6) and the normalization condition

$$\int_{-L/2}^{L/2} ds\ g_q(s)^2 = 1. \tag{9}$$

Then the dynamics of the chain can then be decomposed as

$$\mathbf{r}(s,t) = \sum_{q=0}^{\infty} \mathbf{a}_q(t) g_q(s), \tag{10}$$

where the normal mode amplitudes $\mathbf{a}_q(t)$ are independent of each other and satisfy the Langevin equation:

$$\partial_t \mathbf{a}_q(t) = -\lambda_q \mathbf{a}_q(t) + \tilde{\mathbf{f}}_q(t), \tag{11}$$

$$\langle \tilde{f}_{q\alpha}(t) \tilde{f}_{q'\beta}(t') \rangle = 2k_B T \gamma^{-1} \delta(t-t') \delta_{qq'} \delta_{\alpha\beta}. \tag{12}$$

The vector joining the two reactive monomers can also be written as a linear combination of eigenmodes:

$$\mathbf{R}(t) = \sum_{q \geqslant 1} b_q(s_1,s_2)\ \mathbf{a}_q(t), \tag{13}$$

where the coefficients $b_q(s_1,s_2)$ are simply deduced from the values of the eigenfunctions at positions s_1 and s_2:

$$b_q(s_1,s_2) = g_q(s_1) - g_q(s_2). \tag{14}$$

From Eq. (11), it is straightforward to calculate the correlation between the eigenmodes:

$$\langle \mathbf{a}_q(t).\mathbf{a}_{q'}(0) \rangle = \delta_{qq'} \frac{3k_B T}{\gamma \lambda_q} e^{-\lambda_q t}. \tag{15}$$

Using Eqs (13) and (15), we deduce the value of the normalized autocorrelation function $\phi(t)$ of the vector $\mathbf{R}(t)$:

$$\phi(t) \equiv \frac{\langle \mathbf{R}(t)\mathbf{R}(0) \rangle}{R_{\rm eq}^2} = \frac{3k_B T}{\gamma R_{\rm eq}^2} \sum_{q \geqslant 1} \frac{b_q^2}{\lambda_q} e^{-\lambda_q t}, \tag{16}$$

where $R_{\rm eq}^2 = \langle \mathbf{R}^2 \rangle$ in our Gaussian model has the same expression as in the wormlike chain model [38]:

$$R_{\rm eq}^2 = 2\big[|s_1 - s_2| L_p - L_p^2 (1 - e^{-|s_1-s_2|/L_p})\big]. \tag{17}$$

The autocorrelation function $\phi(t)$ is normalized such that $\phi(0) = 1$ and has the following meaning: if at time $t = 0$ the vector $\mathbf{R}$ is observed to have a value $\mathbf{R}_0$, then at later times t its value is on average $\langle \mathbf{R}(t) \rangle = \mathbf{R}_0 \phi(t)$. We also define $\psi(t)$, as the variance of each coordinate of $\mathbf{R}$ at t, given that $\mathbf{R}(0)$ has some well-defined initial value $\mathbf{R}_0$, and that the rest of the chain is initially at equilibrium:

$$\psi(t) = \langle [\mathbf{R}(t) - \phi(t)\mathbf{R}_0]^2 \rangle / 3. \tag{18}$$

Taking into account the definition (16) of $\phi(t)$, we obtain

$$\psi(t) = R_{\rm eq}^2 [1 - \phi(t)^2]/3. \tag{19}$$

The functions $\psi(t)$ and $\phi(t)$ encode the dynamics of the vector $\mathbf{R}(t)$ at all time scales, and their asymptotics in various limiting cases will be described in the next section.

B. Large eigenvalues and short time behavior of the mean square displacement function

Here we identify the asymptotic behavior of eigenfunctions $g(s)$ associated with large eigenvalues $\lambda \to \infty$. These eigenfunctions vary rapidly with the position s, and we therefore define a rescaled position variable, $u = s(\alpha\lambda_q)^\beta$ with β an exponent and α a scaling factor that will be determined below. We write $g(s) = \tilde{g}(u)$, which we insert into the definition (8) of the eigenfunctions, where we keep only the leading order terms when $\lambda \to \infty$:

$$L_p^4 (\alpha\lambda)^{4\beta} \partial_u^4 \tilde{g}(u) = (\tau_c \lambda) \tilde{g}(u). \tag{20}$$

From this equation, we see that the expansion is consistent for $\lambda \to \infty$ if we set the exponent $\beta = 1/4$, and the scaling factor $\alpha = \tau_c / L_p^4$. The equation for $\tilde{g}(u)$ is simply $(\partial_u^4 - 1)\tilde{g}(u) = 0$, whose solutions can be separated into odd and even eigenfunctions. The even eigenfunctions take the form

$$\tilde{g}(u) = A \cos(u) + B \cosh(u). \tag{21}$$

The boundary conditions (6) are also simplified for large λ: we obtain $\partial_u^3 \tilde{g} = \partial_u^2 \tilde{g} = 0$ at the positions $u = \pm L(\tau_c\lambda)^{1/4}/2L_p$. Inserting these boundary conditions into Eq. (21), we obtain

$$\cos\left[\frac{L(\tau_c\lambda)^{1/4}}{2L_p}\right] \sinh\left[\frac{L(\tau_c\lambda)^{1/4}}{2L_p}\right] + \sin\left[\frac{L(\tau_c\lambda)^{1/4}}{2L_p}\right] \cosh\left[\frac{L(\tau_c\lambda)^{1/4}}{2L_p}\right] = 0. \tag{22}$$

For large values of λ, the solutions of this equation are

$$\frac{L(\lambda\tau_c)^{1/4}}{2L_p} = -\frac{\pi}{4} + n\pi, \tag{23}$$

where n is a positive integer. Taking into account the boundary conditions and the normalization condition (9), the expression of the corresponding even eigenfunction is

$$\tilde{g}(u) \simeq \sqrt{\frac{2}{L}} \left[\cos(u) + \sqrt{2} \cosh(u) e^{-\frac{L(\tau_c\lambda)^{1/4}}{2L_p}} \right], \tag{24}$$

where the cosh term is negligible everywhere except near the boundaries. The odd eigenfunctions can be identified in the same way, and we can gather the results by identifying the asymptotic form taken by the large eigenvalues:

$$\lambda_q \simeq \frac{(q - 1/2)^4 \pi^4}{\tau_c\ \ell^4}, \tag{25}$$

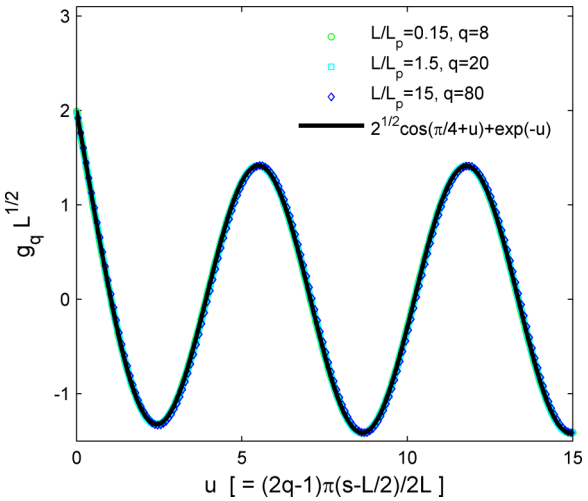

FIG. 2. (Color online) Eigenfunctions close from a boundary in the bending regime, as a function of the variable $u = \pi(2q-1)(L/2-s)/2L$, together with the theoretical prediction (26). The eigenvectors were obtained numerically from the discrete model with $N = 3000$ beads.

while the associated normalized eigenfunctions read

$$g_q(s) \simeq \sqrt{\frac{1}{L}}\left\{\sqrt{2}\,\cos\left[\frac{\pi}{4}+\frac{\pi(2q-1)(L-2s)}{4L}\right] + e^{-\pi(2q-1)\frac{(L-2s)}{4L}} + (-1)^q e^{-\pi(2q-1)\frac{(L+2s)}{4L}}\right\}. \quad (26)$$

In Fig. 2 we represent several eigenfunctions obtained numerically, which all collapse to a single curve, as predicted by Eq. (26), thereby proving that our expansion is correct. The eigenfunctions in this regime are essentially cosine functions, except for a correction near the boundaries, where the exponential correction matters. Since our expansion is valid when $g_q(s)$ varies more rapidly than the two other length scales of the problem, L_p and L, its validity regime is $q \gg 1$ and $q \gg L/L_p$. We note that (25) is identical to the expression of the eigenvalues given in Ref. [32] in the "weakly bending regime," that is, in the limit of short chains, $L/L_p \to 0$ (at fixed q). This could be surprising since our expression (25) is only true asymptotically, in the limit $q \to \infty$. However, we found that in the limit of small L, the expression (25) is already an excellent approximation for the second eigenvalue, with an error made of less than 1.5%, while the error for λ_3 is only 0.04%. Our expansion makes it clear that the eigenfunctions given by Eqs. (25) and (26) are valid for large q, be it for either short ($L \ll L_p$) or long ($L \gg L_p$) chains, and characterize the small-length scale-bending fluctuations in both cases.

The modes with large q characterize the small length scales fluctuations and are associated to an anomalous behavior of the mean square displacement function $\psi(t)$, which can be written from Eqs. (16) and (19) as

$$\psi(t) = \frac{k_B T[1+\phi(t)]}{\gamma}\sum_{q\geqslant 1}\frac{b_q^2(1-e^{-\lambda_q t})}{\lambda_q}. \quad (27)$$

For small times, this series is dominated by the asymptotics of the large eigenvalues (16). Remembering that $\phi(0) = 1$, the following expression is valid at leading order in t:

$$\psi(t) \simeq \frac{4L^4}{3L_p}\sum_{q=q_{\min}}^{\infty}\frac{b_q^2(1-e^{-q^4\pi^4 t/\tau_c \ell^4})}{\pi^4 q^4}, \quad (28)$$

where we have used Eq. (5), and where the sum starts at $q_{\min} \simeq \max(\ell,1)$. In Eq. (28), the coefficient b_q^2 varies much more rapidly with q than the other terms and can be replaced by its value $\overline{b_q^2}$ averaged over neighboring values of q, which can be deduced by considering the definition (14) and the explicit form of the eigenfunctions (26):

$$\overline{b_q^2} \simeq \frac{\beta_b}{L}; \quad \beta_b = \begin{cases} 8 & \text{if} \quad s_2 = L/2 = -s_1, \\ 5 & \text{if} \quad -L/2 < s_1 < s_2 = L/2 \\ 2 & \text{if} \quad -L/2 < s_1 < s_2 < L/2. \end{cases}. \quad (29)$$

Then the series (28) is well approximated by the following integral, obtained by defining $y = q(t/\tau_c)^{1/4}/\ell$:

$$\psi(t) \simeq \frac{4L_p^2\beta_b}{3}\left(\frac{t}{\tau_c}\right)^{3/4}\int_0^\infty dy\,\frac{(1-e^{-y^4\pi^4})}{\pi^4 y^4}. \quad (30)$$

This integral can be evaluated analytically:

$$\psi(t) \simeq \frac{4\Gamma(1/4)\beta_b}{9\pi}L_p^2\left(\frac{t}{\tau_c}\right)^{3/4} \equiv \kappa\, t^{3/4}, \quad (31)$$

where $\Gamma(.)$ is the Gamma function. This regime characterizes the subdiffusion at small times scales due to the small length scale bending fluctuations. Note that the effect of monomer position is entirely taken into account through the coefficient β_b, and this formula predicts that the motion of the end monomers is enhanced. Although the scaling $t^{3/4}$ has been identified in previous works (for circular chains in Ref. [33], and averaged over the monomer positions in Ref. [39]), the dependence of the prefactor κ with the monomer positions has not been identified before. The same scaling holds for the perpendicular displacements of the slightly bent inextensible wormlike chains; see, e.g., Ref. [27].

C. Other dynamic regimes

Additionally to the subdiffusive regime (31) due to small-scale bending fluctuations, other regimes emerge for $\psi(t)$ in the limit of short chains ($\ell \to 0$) and long chains ($\ell \to \infty$). We describe these regimes now and summarize them in Fig. 3.

The asymptotics of the eigenvalues are well known in the limit $\ell \to \infty$ and $\ell \to 0$ for a fixed value of q, that is, for a fixed value of the length scale. In the limit of long chains (or short persistence length $L_p \to 0$), the eigenfunctions can be readily identified by keeping the leading order terms in Eq. (8), from which we get $L_p^2\partial_s^2 g(s) = -\lambda\tau_c g(s)$, and the boundary conditions (6) simplify into $\partial_s g = 0$ for $s = \pm L/2$. Consequently, we readily obtain that the eigenfunctions are those of the Rouse model,

$$\lambda_q = \frac{q^2\pi^2}{\tau_c\,\ell^2}, \quad g_q(s) = \sqrt{\frac{2}{L}}\cos\left[\frac{q\pi(L/2-s)}{L}\right]. \quad (32)$$

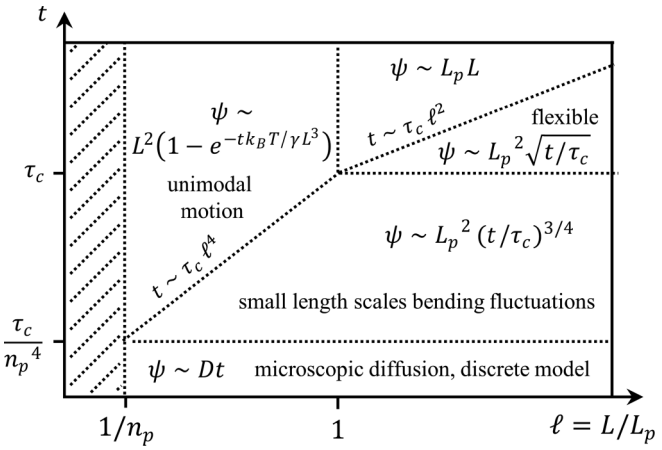

FIG. 3. Summary of all the regimes for the mean square displacement function $\psi(t)$ described by Eqs. (31), (34), (37), and (36). The dashed area region corresponds to a polymer with less than one monomer and is meaningless. Scales are logarithmic, and numerical coefficients are not written in this figure. n_p represents the number of beads per persistence length in the discrete model, $n_p = N/\ell$.

We define the average of the coefficients b_q^2 over neighboring values of q:

$$\overline{b_q^2}(s_1,s_2) = \frac{\beta_e}{L}; \quad \beta_e = \begin{cases} 4 & \text{(exterior-exterior)} \\ 3 & \text{(exterior-interior)} \\ 2 & \text{(interior-interior).} \end{cases} \tag{33}$$

Inserting (32) and (33) into the the series (27) and transforming the resulting series into an integral, we obtain the anomalous diffusive behavior characteristics of long (Rouse) chains:

$$\psi(t) \simeq \frac{4\beta_e L_p^2}{3\sqrt{\pi}} \left(\frac{t}{\tau_c}\right)^{1/2}. \tag{34}$$

In the opposite limit of short chains, $\ell \to 0$, there is essentially one eigenvalue which is much smaller than the others, associated to the global rotational and extensional degree of freedom of the chain. The first eigenvalue and the corresponding eigenvector in this regime are given by [32]

$$\lambda_1 = \frac{24}{\tau_c \ell^3} = \frac{36 k_B T}{\gamma L^3}, \quad g_1(s) = \pm \frac{\sqrt{12}}{L^{3/2}} s. \tag{35}$$

The time scale $\lambda_1^{-1} \simeq L^3$ in this regime is of the order of the rotational time of a rigid rod of length L. The other eigenvalues are of order $O(\ell^{-4})$ and their dynamics is much faster than that of the first mode. The corresponding mean square displacement function is

$$\psi(t) \simeq \frac{|s_1 - s_2|^2}{3} [1 - e^{-48t/(\tau_c \ell^3)}]. \tag{36}$$

In this regime, the monomers behave as if they were linked by a single spring, as a result of a contractional degree of freedom in this Gaussian model that has the same value as the rotational relaxation time scales. This regime can be termed "unimodal motion," since only one mode contributes to the dynamics.

Finally, if the number of beads N in the chain is finite, as in the discrete model, there is one regime for small time scales where the monomers do not feel their neighbors and diffuse freely, as can be seen by considering Eq. (2). In this regime, the mean square displacement function reads

$$\psi(t) \simeq 4Dt \ (t \to 0, \text{fixed } N), \tag{37}$$

where $D = k_B T/\zeta$ is the diffusion coefficients of individual monomers in the discrete model.

The different dynamical regimes, given by Eqs. (31), (34), (37), and (36), are reported in Fig. 3, where one can easily see the validity domain of each of these expressions.

IV. MEAN CYCLIZATION TIME

A. Markovian approach

We now identify all the regimes of cyclization time in the Gaussian semiflexible model: we determine the mean first passage time, $\langle \mathbf{T} \rangle$, that the vector $\mathbf{R}(t)$ joining the reactive monomers reaches the reactive region: $|\mathbf{R}(t)| < a$ with a the capture radius. We first make use of a Wilemski-Fixman (WF) -type approach, which neglects memory effects. Let us assume that initially the polymer is at equilibrium and that the capture radius is initially so small that we can neglect the probability to be inside the reactive region at $t = 0$. We call P_S the equilibrium probability density to observe $\mathbf{R} = \mathbf{0}$. Let us call $f(\{\mathbf{a}\},t)$ the probability density that the first passage to the reactive region occurs at time t, with a polymer configuration $\{\mathbf{a}\} = (\mathbf{a}_1, \mathbf{a}_2, \ldots)$. By partitioning over the first passage events, we write the renewal equation [40]

$$P_S = \int_0^t dt' \int d\{\mathbf{a}'\} f(t', \{\mathbf{a}'\}) P(\mathbf{0}, t - t' | \{\mathbf{a}'\}, 0). \tag{38}$$

Taking the temporal Laplace transform and expanding for small values of the Laplace variable leads to [19]

$$\langle \mathbf{T} \rangle P_S = \int_0^\infty dt [P(\mathbf{0}, t | \pi, 0) - P_S], \tag{39}$$

where $P(\mathbf{0}, t | \pi, 0)$ represents the probability to observe $\mathbf{R} = \mathbf{0}$ at time t, given that at time 0 the distribution of polymer conformations is $\pi(\{\mathbf{a}\}) \equiv \int_0^\infty dt f(t, \{\mathbf{a}\})$. As shown in Refs. [11,19,21], in the Wilemski-Fixman approach, the distribution of reactive conformations is approximated by an equilibrium distribution of modes, with the constraint that $|\mathbf{R}| = a$. We remind that, if a chain at equilibrium at time $t = 0$ is observed with a value $\mathbf{R}_0$ for the reactive vector, then the average of $\mathbf{R}$ at t is $\mathbf{R}_0 \phi(t)$ and the variance of each coordinate is $\psi(t)$. Hence, in the Wilemski-Fixman approximation, Eq. (39) becomes

$$\langle \mathbf{T} \rangle_{\mathrm{WF}} P_S = \int_0^\infty dt \left\{ \frac{e^{-a^2 \phi(t)^2 / 2\psi(t)}}{[2\pi \psi(t)]^{3/2}} - P_S \right\}, \tag{40}$$

as shown for example in Ref. [20]. In Eq. (40), the quantity P_S is the equilibrium contact probability density of the two reactive monomers, that is, the probability density that $\mathbf{R} = \mathbf{0}$, given by $P_S = [3/2\pi R_{\mathrm{eq}}^2]^{3/2}$. Note that the Wilemski-Fixman approach takes into account the dynamics at all time scales through the dynamical functions $\phi(t)$ and $\psi(t)$ and can be reasonably used to identify the asymptotics of the mean reaction time in limiting regimes. However, this approach is Markovian and neglects memory effects, which can lead to

quantitative overestimates of the reaction time [19,20], as we will show in Sec. IV B.

Let us focus on the limit of small reactive radius ($a \to 0$). In this limit, the integral in Eq. (40) is controlled by the short time behavior $\psi \sim \kappa t^{3/4}$, so that

$$\langle \mathbf{T} \rangle_{\mathrm{WF}} P_S \simeq \int_0^\infty dt \frac{1}{[2\pi\kappa t^{3/4}]^{3/2}} e^{-a^2/(2\kappa t^{3/4})}. \quad (41)$$

An analytical evaluation of this formula gives

$$\langle \mathbf{T} \rangle_{\mathrm{WF}} \simeq \frac{3^{7/6}\sqrt{2}\pi^{4/3}\Gamma(7/6)}{\Gamma(1/4)^{4/3}} \times \frac{R_{\mathrm{eq}}^3 \tau_c}{\beta^{4/3} a^{1/3} L_p^{8/3}}. \quad (42)$$

In this regime $a \to 0$, the mean reaction time is controlled by the small-length scale bending fluctuations, which leads to novel scalings with a and L_p. The effect of the relative positions of the monomers is taken into account through R_{eq} and β_b. This expression shows that the reaction will be 6.3 times faster for the two extremal monomers than for two monomers in the bulk of the chain (assuming an identical curvilinear distance between reactive monomers). This increase of the reaction rate for extremal monomers is due to the fact that fluctuations are more important at these ends. The similar scaling $\langle \mathbf{T} \rangle \sim a^{-1/3}$ was already derived by Berg [34] in the case of a monomer of a circular semiflexible chain reacting with an external target. The exponent $-1/3$ can be understood by considering that the problem is equivalent to the search of a target of size a in an effective volume P_S^{-1}, the walker having a walk dimension [defined by $\psi(t) = t^{2/d_w}$], $d_w = 8/3$. In this case, the fact that d_w is smaller than the spatial dimension ($d = 3$) implies that the search time is controlled by the target size [41,42] and that $\langle \mathbf{T} \rangle \sim a^{d_w - d}$, consistent with the result in Eq. (42).

Depending on the respective values of a and L, other regimes emerge, as summarized in Fig. 4. For long chains $\ell \to \infty$, the mean cyclization time scales as

$$\langle \mathbf{T} \rangle_{\mathrm{WF}} \sim \tau_c \ell^2, \quad (43)$$

as in the case of a continuous flexible chain. For short chains $\ell \ll 1$, the dynamics is controlled by the first mode only, so that it is equivalent to a single spring. As a consequence, the mean cyclization time reads

$$\langle \mathbf{T} \rangle_{\mathrm{WF}} \simeq P_S^{-1} \int_0^\infty dt \frac{e^{-a^2\tau_c\ell^3/(32|s_1-s_2|^2 t)}}{[32\pi|s_1-s_2|^2 t/(\tau_c \ell^3)]^{3/2}}. \quad (44)$$

This expression can be simplified:

$$\langle \mathbf{T} \rangle_{\mathrm{WF}} \simeq \sqrt{\frac{\pi}{6}} \frac{L^3 \gamma |s_1 - s_2|}{36\, a\, k_B T}. \quad (45)$$

This formula is due to the extensible nature of the polymer in the Gaussian model, implying that stretching is favored compared to bending to make a contact between the two ends. The $1/a$ dependence of $\langle \mathbf{T} \rangle$ is characteristic of diffusive search in a three-dimensional space.

Finally, in the discrete model where $n_p = N/\ell$ denotes the number of monomers per persistence length, the continuous description becomes irrelevant for $a < L_p/n_p^{3/2}$, and the kinetics is controlled by finite size effects independent of bending. In this regime, the mean cyclization time is controlled by the microscopic diffusion coefficient D of individual monomers at short time scales,

$$\langle \mathbf{T} \rangle_{\mathrm{WF}} \simeq P_S^{-1} \int_0^\infty dt \frac{e^{-a^2/(8Dt)}}{[8\pi Dt]^{3/2}} = \frac{\pi^{1/2} R_{\mathrm{eq}}^3}{6\sqrt{6}\, a D} \quad (46)$$

and scales as $\langle \mathbf{T} \rangle \simeq R_{\mathrm{eq}}^3/Da$. Again, the $1/a$ dependence of $\langle \mathbf{T} \rangle$ is linked to the fact that the motion is purely diffusive at this scale. In this regime, the reactive monomers behave as independent Brownian walkers moving in a space of effective volume P_S^{-1}, leading to Eq. (46), which is exactly the same as in the case of discrete Rouse polymers in the limit $a \to 0$ [11,17,19,20].

We illustrate the dependence of the mean reaction time with the contour length in the continuous regime in Fig. 5, where it is observed that, for small values of a, the mean reaction time is

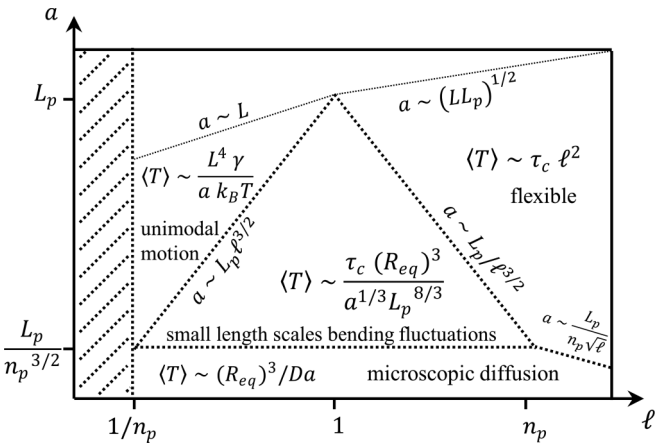

FIG. 4. Summary of the regimes of end-to-end cyclization described by Eqs. (42), (43), (45), and (46).

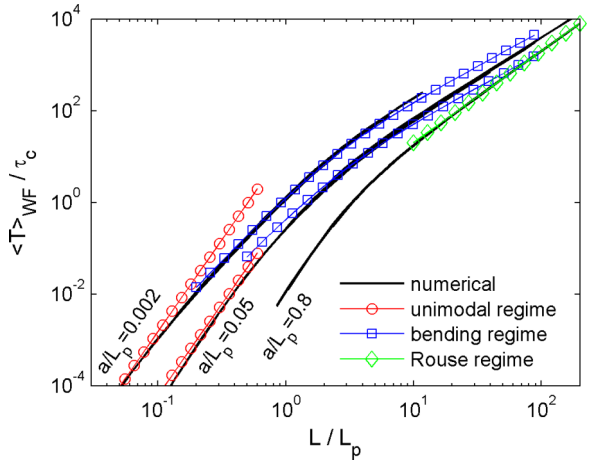

FIG. 5. (Color online) End-to-end cyclization time of continuous semiflexible chains in the Wilemski-Fixman approximation for three different values of a/L_p. Curves are obtained from the analysis of the discrete model; the number of beads is always chosen so that the continuous regime is reached (for practical reasons, we require that $N = n_p \ell \leqslant 3000$, which prevents us to explore the regime of long polymers with small capture radius). Curves corresponding to asymptotic regimes are also shown ["unimodal" regime: Eq. (45), "bending" regime: Eq. (42), "Rouse" regime Eq. (43)].

first given by the stiff regime formula for small polymer length, then passes through the bending regime for intermediate values of ℓ, and then becomes asymptotically equal to its value in the Rouse regime. It should be noted that, the smaller the capture radius, the larger the contour length must be to observe the Rouse regime. For example, for $a = 0.002L_p$, the cyclization time is comparable to its value in the Rouse regime only if the contour length exceeds a few hundreds of persistence lengths.

B. Mean cyclization time: Non-Markovian effects in the bending regime

Up to now, we have considered the results of the Wilemski-Fixman theory, whose main assumption is that the distribution of reactive conformations is an equilibrium distribution. The non-Markovian effects in the Rouse regime have been investigated in detail in previous works [19,20], where they lead to a quantitative decrease of the reaction time for long chains by a factor of 20%–50% according to the value of the capture radius. They have also been found to be negligible in the finite size regime, because in this regime only the short time diffusive behavior of $\mathbf{R}(t)$ matters, which is Markovian. We also expect that non-Markovian effects are negligible in the stiff limit, where there is only one relaxation time and the problem becomes Markovian. Therefore, we focus here only on the characterization of the non-Markovian effects in the bending regime, $a \to 0$ and ℓ finite. We make use of a theory that was proposed recently [19,20], in which the main assumption is that the distribution of reactive conformations is a multivariate Gaussian distribution, whose moments are to be determined by solving a set of self-consistent equations.

More precisely, we define the direction of reaction as being the spatial orientation $\hat{\mathbf{u}}$ of the vector $\mathbf{R}$ at the instant of reaction. We assume that, at the instant of first contact, the modes $\mathbf{a}_q$ have an average value m_q^π in the direction $\hat{\mathbf{u}}$, and that their average is 0 in the two other perpendicular directions. For simplicity, we also assume that the covariance matrix of the modes $\mathbf{a}_q$ is given by its equilibrium value. The values of the modes m_q^π are defined by a set of self-consistent equations, obtained by multiplying Eq. (39) by $\mathbf{a}_q^\pi \delta(\mathbf{R} - \sum_q b_q \mathbf{a}_q)$ and integrating over all conformations. The result of this calculation is [20]

$$\int_0^\infty dt \frac{e^{-R_\pi(t)^2/2\psi(t)}}{\psi(t)^{5/2}} \left\{ \frac{\mu_q^{\pi,0} R_\pi(t)}{3} + \frac{b_q \phi(t)[\phi(t) - e^{-\lambda_q t}]}{\lambda_q} \right\} = 0, \tag{47}$$

where $\mu_q^{\pi,0}$ and $R_\pi(t)$ read

$$\mu_q^{\pi,0} = m_q^\pi e^{-\lambda_q t} - \frac{R_\pi(t) b_q [1 - \phi(t) e^{-\lambda_q t}]}{\lambda_q \psi(t)}, \tag{48}$$

$$R_\pi(t) = a - \sum_{q \geqslant 1} b_q m_q^\pi (1 - e^{-\lambda_q t}). \tag{49}$$

The quantity $R_\pi(t)$ represents physically the average position of the vector $\mathbf{R}$ at a time t after the first passage, in the direction $\hat{\mathbf{u}}$ [20]. Equations (47) and (48) are exactly Eqs. (30) and (31) of Ref. [20], in which the terms containing the functions "Z" and "G" (in the notations of Ref. [20]) have been omitted, which is justified in the limit $a \ll R_{\rm eq}$.

In the non-Markovian theory, the mean reaction time can be calculated by integrating Eq. (39) over all configurations $\{\mathbf{a}\}$ satisfying $\sum_q b_q \mathbf{a}_q = \mathbf{R}$ and can therefore be written as [20]

$$\langle \mathbf{T} \rangle P_S = \int_0^\infty dt \left\{ \frac{e^{-[R_\pi(t)]^2/2\psi(t)}}{[2\pi\psi(t)]^{3/2}} - P_S \right\}. \tag{50}$$

This expression is similar to the corresponding expression in the Wilemski-Fixman approximation (40), but now involves the reactive trajectory $R_\pi(t)$. We note that the multiplication of Eq. (47) by $b_q e^{-\lambda_q \tau}$ for some positive τ leads to a single equation for the reactive trajectory:

$$\int_0^\infty dt \left\{ R_\pi(t) R_\pi(t+\tau) - \frac{R_\pi(t)^2 R_{\rm eq}^2 [\phi(\tau) - \phi(t)\phi(t+\tau)]}{3\psi(t)} + \phi(t) R_{\rm eq}^2 [\phi(t)\phi(\tau) - \phi(t+\tau)] \right\} \frac{e^{-\frac{[R_\pi(t)]^2}{2\psi(t)}}}{\psi(t)^{5/2}} = 0, \tag{51}$$

which must be satisfied for all $\tau > 0$ with the boundary condition $R_\pi(0) = a$. Hence, the variables m_q^π have been eliminated. We are now going to analyze this equation for $a \to 0$, in order to estimate the magnitude of the non-Markovian effects in the bending regime. We introduce the characteristic time scale in the bending regime $t^* = a^{8/3}/\kappa^{4/3}$, where κ was defined in (31), and we set $\tilde{t} = t/t^*$, and $\tilde{\tau} = \tau/t^*$. Introducing the scaling function h defined by

$$R_\pi(t) = a\, h(t/t^*), \quad t^* = a^{8/3}/\kappa^{4/3}, \tag{52}$$

Eq. (51) leads to lowest order in $a \to 0$ to

$$\int_0^\infty \frac{d\tilde{t}}{\tilde{t}^{15/8}} e^{-h(\tilde{t})^2/2\tilde{t}^{3/4}} \left\{ h(\tilde{t})[h(\tilde{t}+\tilde{\tau}) - h(\tilde{t})] + \frac{3}{2}\left[(\tilde{t}+\tilde{\tau})^{\frac{3}{4}} - \tilde{t}^{\frac{3}{4}} - \tilde{\tau}^{\frac{3}{4}}\right]\left[1 - \frac{h(\tilde{t})^2}{3\,\tilde{t}^{\frac{3}{4}}}\right] \right\} = 0. \tag{53}$$

This equation fully determines $h(\tilde{t})$ and was solved numerically. The result is represented in Fig. 6, which shows that $R_\pi(t)$ sharply increases at short times (as compared to the time scale t^*) before saturating to a plateau [the analysis of the properties of Eq. (53) shows that the behavior of $h(t)$ for $t \to \infty$ is $h(t) \simeq A + B/t^{1/8}$].

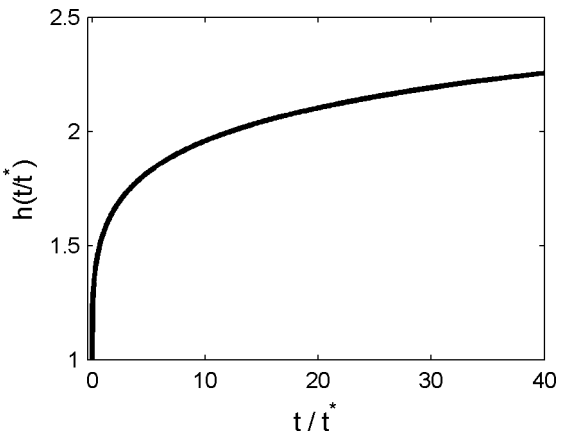

FIG. 6. Numerical solution $h(\tilde{t}) = h(t/t^*)$ of the nonlinear integral equation (53), representing the rescaled reactive trajectory (see text).

Rewriting Eq. (50) in the limit $a \to 0$ in terms of h yields

$$\langle \mathbf{T} \rangle P_S \simeq \frac{\kappa^{-4/3}}{(2\pi)^{3/2} a^{1/3}} \int_0^\infty \frac{d\tilde{t}}{\tilde{t}^{\,9/8}} \exp\left[-\frac{h(\tilde{t})^2}{2\,\tilde{t}^{\,3/4}} \right]. \quad (54)$$

Thus, the non-Markovian effects do not change the influence of the positions of the reactive monomers on the mean cyclization time. Using our numerical evaluation of h, we find that

$$\langle \mathbf{T} \rangle \simeq 3.3 \times \frac{R_{\rm eq}^3 \tau_c}{\beta_b^{4/3} a^{1/3} L_p^{8/3}}. \quad (55)$$

Comparing with the formula (42) in the Wilemski-Fixman approximation, we observe that the magnitude of the non-Markovian effects in the mean reaction time are of the order of 18% in the bending regime.

C. Numerical stochastic simulations

Finally, in order to test the capability of the theory to deal with non-Markovian effects, we performed numerical stochastic simulations of the Langevin equation (2) in the case that the polymer is formed by a finite number of beads. Simulations to obtain the mean first contact time between the two end monomers were performed by using the Ermak algorithm [43]. In short, we used a constant time step Δt, and if $(x_{i,k}, y_{i,k}, z_{i,k})$ represent the coordinates of the position of the ith monomer at the kth time step, the positions at the $(k+1)$th step are deduced from the equation:

$$x_{i,k+1} = x_{i,k} + \frac{\Delta t}{\zeta} \sum_{j=1}^{N} A_{ij} x_{j,k} + \sqrt{2D\Delta t}\, u_k, \quad (56)$$

with u_k a list of independent Gaussian random numbers with zero mean and variance 1, and A is the pentadadiagonal matrix such that the force on monomer i is $\mathbf{F}_i = \sum_{j=1}^{N} A_{ij} \mathbf{r}_j$, so that the elements $A_{ij} = \partial_{x_i} \partial_{x_j} V$ are deduced from the potential V in Eq. (1). The other coordinates y_i and z_i of all the monomers evolve through the same equation as Eq. (56). At each step, we compare $|\mathbf{r}_N - \mathbf{r}_1|$ to the value of the capture radius a, if it is smaller the simulation stops and the current time is recorded. The simulations are always performed with a time Δt at least 10 times smaller than the inverse of the largest eigenvalue of A/ζ, in order to be sure to seize all the time scales of the polymer dynamics. The algorithm was used for smaller and smaller values of the time steps in order to be sure that the final results for the mean first passage time do not depend on the time step used.

The results of the simulations are presented in Table I for several values of parameters for finite numbers of beads N. In this table, they are compared with the predictions of the non-Markovian theory, which are determined by solving numerically Eqs. (47) and (48) written for a finite number of beads [more precisely, the equations to be solved are exactly Eqs. (30) and (31) of Ref. [20], where one uses the eigenvalues and eigenvectors of the dynamical matrix of the semiflexible chain]. We also report the predictions of the Wilemski-Fixman theory in Table I.

Comparison between theory and simulation reveals that the Wilemski-Fixman systematically overestimates the mean cyclization time. This is consistent with the general considerations of Portman *et al.* [44,45], who showed that Wilemski-Fixman approach provides an upper bound on the mean cyclization time. In turn, Table I clearly shows that the result of the non-Markovian theory are in quantitative agreement with the simulations for all the tested values of a, ℓ, N, and L_p. The precision is of the order of the percent, and we infer that our non-Markovian effects are correctly estimated by our theory.

TABLE I. Results of stochastic simulations of end-to-end cyclization ($\langle \mathbf{T} \rangle_{\rm simu}$) of the Gaussian discrete semiflexible chain of N beads described by Eqs. (1) and (2), compared to the predictions of the (Markovian) Wilemski-Fixman theory ($\langle \mathbf{T} \rangle_{\rm WF}$) and the non-Markovian theory ($\langle \mathbf{T} \rangle_{\rm NM}$) for the same parameters.

a/L_p	ℓ	N	$\langle \mathbf{T} \rangle_{\rm simu}/\tau_c$	$\langle \mathbf{T} \rangle_{\rm NM}/\tau_c$	$\langle \mathbf{T} \rangle_{\rm WF}/\tau_c$
0.2	5	25	7.3 ± 0.1	7.33	8.62
0.2	1	5	0.0615 ± 0.0005	0.0611	0.0648
0.2	1	10	0.0652 ± 0.0005	0.0654	0.0752
0.2	1	20	0.064 ± 0.001	0.06601	0.0798
0.1	1	10	0.132 ± 0.006	0.134	0.156
0.01	0.1	10	$(2.222 \pm 0.002)10^{-4}$	2.224×10^{-4}	2.417×10^{-4}

V. CONCLUSION

Let us now summarize our findings. In this paper, we have focused on the impact of the complex, collective dynamics of a semiflexible chain on the mean cyclization time. We have used a simplified (Gaussian) description of semiflexible chains, where the inextensibility of the chain constraint holds only on average. We have derived all the different dynamical regimes, arising from the multiplicity of length scales in the problem, and derived the corresponding regimes of the cyclization time, as summarized in Fig. 4. The asymptotic results for the mean reaction time were first derived in the framework of the Wilemski-Fixman theory, where the complex dynamics of the chain is partly taken into account, with the assumptions that the relative motion of two monomers is Markovian. Then, we evaluated the importance of non-Markovian effects by using the recent method introduced in Refs. [19,20], which takes into account the impact of the (nonequilibrium) configuration of the chains at the instant of the reaction. These non-Markovian effects were proved to be quantitatively important ($\simeq$18%) in the regime controlled by the small length scale bending fluctuations. Non-Markovian effects are also important in the previously studied regime of flexible (Rouse) chains, giving numerical factors around 1–2 for the mean cyclization time, but are unimportant in all other limiting cases, which are controlled by diffusion. Thus, we could quantify precisely the magnitude of non-Markovian effects in all limiting cases. Comparison with Brownian dynamics simulations of the Gaussian model for finite numbers of beads shows that our analysis of the non-Markovian effects is accurate.

In the regime controlled by small length scale bending fluctuations, the cyclization time varies with the capture radius as $\langle \mathbf{T} \rangle \sim a^{-1/3}$. Notably, we could seize the dependence of the prefactor with the monomer positions, leading the prediction that the cyclization time between two interior monomers is more than six times faster than for monomers located at the chain ends. This strong dependence of the reaction time with the positions of the reactive monomers is the same in

the Marvovian and non-Markovian theories. We could also describe the effect of having a chain with a finite number of beads on the cyclization time. Due to the fact that, at very small time scales, individual monomers behave as free Brownian walkers, the behavior $\langle \mathbf{T} \rangle \sim a^{-1/3}$ breaks down and becomes $\langle \mathbf{T} \rangle \sim 1/a$. This means that, in a simulation, the smaller the capture radius, the larger the number of beads must be in order to describe the regime controlled by small length scales bending fluctuations.

The main limitation of this model is that it does not take rigorously into account the inextensibility constraint of the wormlike chain model. As a consequence, the probability to be in contact, P_S, is not correctly evaluated in the limit of short chains in our Gaussian model, which cannot take into account the energy cost for making a loop in a stiff rod. However, for long chains the results for the cyclization time are expected to be valid, and to properly take into account bending fluctuations. Interestingly, numerical simulations of the cyclization of inextensible chains [30] have revealed regimes where $\langle \mathbf{T} \rangle$ varies slower with a than a^{-1}, to be compared with the $a^{-1/3}$ regime predicted by our theory. In the case of short chains, our study still reveals that, when the size of the capture radius is not infinitely small, the rotational diffusion of the chain should play a role in the cyclization, giving rise to regimes that differ from the $1/a^{1/3}$ dependence.

In conclusion, although we presented a simplified description of semiflexible chains, it still exhibits a large number of time and length scales, which give rise to complex cyclization regimes that are richer than previously recognized. There is a need for analysis that would take into account both inextensibility constraints and the collective dynamics of the polymer chain. Such theories exist for now only for slightly bent chains, not for looping configurations. It is our hope that the present work will help to elucidate the cyclization properties of polymers in more complex models that would take into account the inextensibility or the hydrodynamic interactions in semiflexible chains.

ACKNOWLEDGMENTS

T.G., O.B., and R.V. acknowledge the support of the Campus France (Project No. 28252XE) and of European Research Council starting Grant No. FPTOpt-277998. M.D. and A.B. acknowledge the support of the DAAD through the PROCOPE program (Project No. 55853833), of the DFG through Grant No. Bl 142/11-1, and of the DFG through IRTG "Soft Matter Science" (GRK 1642/1).

[1] G. Bonnet, O. Krichevsky, and A. Libchaber, Proc. Natl. Acad. Sci. USA **95**, 8602 (1998).
[2] M. I. Wallace, L. Ying, S. Balasubramanian, and D. Klenerman, Proc. Natl. Acad. Sci. USA **98**, 5584 (2001).
[3] X. Wang and W. M. Nau, J. Am. Chem. Soc. **126**, 808 (2004).
[4] T. Uzawa, R. R. Cheng, K. J. Cash, D. E. Makarov, and K. W. Plaxco, Biophys. J. **97**, 205 (2009).
[5] L. J. Lapidus, W. A. Eaton, and J. Hofrichter, Proc. Natl. Acad. Sci. USA **97**, 7220 (2000).
[6] A. Möglich, K. Joder, and T. Kiefhaber, Proc. Natl. Acad. Sci. USA **103**, 12394 (2006).
[7] M. Buscaglia, L. J. Lapidus, W. A. Eaton, and J. Hofrichter, Biophys. J. **91**, 276 (2006).
[8] J.-F. Allemand, S. Cocco, N. Douarche, and G. Lia, Eur. Phys. J. E **19**, 293 (2006).
[9] D. Shore, J. Langowski, and R. L. Baldwin, Proc. Natl. Acad. Sci. USA **78**, 4833 (1981).
[10] R. Vafabakhsh and T. Ha, Science **337**, 1097 (2012).
[11] R. Pastor, R. Zwanzig, and A. Szabo, J. Chem. Phys. **105**, 3878 (1996).
[12] G. Wilemski and M. Fixman, J. Chem. Phys. **60**, 866 (1974).
[13] G. Wilemski and M. Fixman, J. Chem. Phys. **60**, 878 (1974).
[14] B. Friedman and B. O'Shaughnessy, Phys. Rev. A **40**, 5950 (1989).
[15] I. M. Sokolov, Phys. Rev. Lett. **90**, 080601 (2003).
[16] N. M. Toan, G. Morrison, C. Hyeon, and D. Thirumalai, J. Phys. Chem. B **112**, 6094 (2008).
[17] A. Amitai, I. Kupka, and D. Holcman, Phys. Rev. Lett. **109**, 108302 (2012).
[18] A. E. Likthman and C. M. Marques, Europhys. Lett. **75**, 971 (2006).
[19] T. Guérin, O. Bénichou, and R. Voituriez, Nat. Chem. **4**, 568 (2012).
[20] T. Guérin, O. Bénichou, and R. Voituriez, J. Chem. Phys. **138**, 094908 (2013).
[21] T. Guérin, O. Bénichou, and R. Voituriez, Phys. Rev. E **87**, 032601 (2013).
[22] N. Saitô, K. Takahashi, and Y. Yunoki, J. Phys. Soc. Jpn. **22**, 219 (1967).
[23] B. Alberts, D. Bray, J. Lewis, M. Raff, K. Roberts, and J. D. Watson, *Molecular Biology of the Cell* (Garland Science, New York, 2008).
[24] J. Howard, *Mechanics of Motor Proteins and the Cytoskeleton* (Sinauer Associates, Sunderland, MA, 2001).
[25] J. Shimada and H. Yamakawa, Macromolecules **17**, 689 (1984).
[26] O. Hallatschek, E. Frey, and K. Kroy, Phys. Rev. E **75**, 031905 (2007).
[27] T. B. Liverpool, Phys. Rev. E **72**, 021805 (2005).
[28] S. Jun, J. Bechhoefer, and B.-Y. Ha, Europhys. Lett. **64**, 420 (2003).
[29] C. Hyeon and D. Thirumalai, J. Chem. Phys. **124**, 104905 (2006).
[30] R. Afra and B. A. Todd, J. Chem. Phys. **138**, 174908 (2013).
[31] M. Bixon and R. Zwanzig, J. Chem. Phys. **68**, 1896 (1978).
[32] L. Harnau, R. G. Winkler, and P. Reineker, J. Chem. Phys. **102**, 7750 (1995).
[33] O. G. Berg, Biopolymers **18**, 2861 (1979).
[34] O. G. Berg, Biopolymers **23**, 1869 (1984).
[35] A. Dua and B. Cherayil, J. Chem. Phys. **117**, 7765 (2002).
[36] A. Dua and B. Cherayil, J. Chem. Phys. **116**, 399 (2002).
[37] M. Doi and S. F. Edwards, *The Theory of Polymer Dynamics* (Clarendon Press, Oxford, 1988).
[38] R. G. Winkler, P. Reineker, and L. Harnau, J. Chem. Phys. **101**, 8119 (1994).

[39] L. Harnau, R. G. Winkler, and P. Reineker, J. Chem. Phys. **106**, 2469 (1997).
[40] N. Van Kampen, *Stochastic Processes in Physics and Chemistry,* 3rd ed. (North-Holland Personal Library, Amsterdam, 1992).
[41] S. Condamin, O. Bénichou, V. Tejedor, R. Voituriez, and J. Klafter, Nature (London) **450**, 77 (2007).
[42] O. Bénichou and R. Voituriez, Phys. Rev. Lett. **100**, 168105 (2008).
[43] D. L. Ermak, J. Chem. Phys. **62**, 4189 (1975).
[44] J. Portman, J. Chem. Phys. **118**, 2381 (2003).
[45] J. J. Portman and P. G. Wolynes, J. Phys. Chem. A **103**, 10602 (1999).